Multigluon Correlations and Evidence of Saturation from Dijet Measurements at an Electron-Ion Collider

Heikki Mäntysaari,[1,2,*] Niklas Mueller,[3,†] Farid Salazar,[3,4,‡] and Björn Schenke[3,§]
[1]Department of Physics, University of Jyväskylä, P.O. Box 35, 40014 University of Jyväskyä, Finland
[2]Helsinki Institute of Physics, P.O. Box 64, 00014 University of Helsinki, Finland
[3]Physics Department, Brookhaven National Laboratory, Building 510A, Upton, New York 11973, USA
[4]Department of Physics and Astronomy, Stony Brook University, Stony Brook, New York 11794, USA

(Received 18 December 2019; revised manuscript received 5 February 2020; accepted 5 February 2020; published 17 March 2020)

We study inclusive and diffractive dijet production in electron-proton and electron-nucleus collisions within the color glass condensate effective field theory. We compute dijet cross sections differentially in both mean dijet transverse momentum $\boldsymbol{P}$ and recoil momentum $\boldsymbol{\Delta}$, as well as the anisotropy in the relative angle between $\boldsymbol{P}$ and $\boldsymbol{\Delta}$. Our results cover a much larger kinematic range than accessible in previous computations performed in the correlation limit approximation, where it is assumed that $|\boldsymbol{P}| \gg |\boldsymbol{\Delta}|$. We validate this approximation in its range of applicability and quantify its failure for $|\boldsymbol{P}| \lesssim |\boldsymbol{\Delta}|$. We also predict significant target-dependent deviations from the correlation limit approximation for $|\boldsymbol{P}| > |\boldsymbol{\Delta}|$ and $|\boldsymbol{P}| \lesssim Q_s$, which offers a straightforward test of gluon saturation and access to multigluon distributions at a future Electron-Ion Collider.

DOI: 10.1103/PhysRevLett.124.112301

Introduction.—To gain a complete understanding of the complex multi-parton structure of nuclei at small x, measurements of a multitude of processes in high energy $e + p(A)$ collisions over a wide range of kinematics are necessary. A future Electron-Ion Collider (EIC) [1–3] will provide an ideal tool for such an endeavor, with dijet production being one of the most important processes to access the structure of gluon fields and their nonlinear dynamics inside protons and heavier nuclei.

While coherent diffractive dijet production allows one to access the target's spatial geometry [4–8], inclusive and incoherent diffractive dijet cross sections are sensitive to multigluon correlations in the target [9,10] (see also [11–15]). In the back-to-back correlation limit approximation (CLA), where the mean dijet momentum is much larger than the recoil momentum, the inclusive dijet production cross section can be expressed in terms of the Weizsäcker-Williams transverse momentum dependent gluon distributions (TMDs), allowing one experimental access to these fundamental quantities [9,16–19]. We advocate going beyond this limit to allow for deeper insights into the multigluon structure of the nucleus. Inclusive and diffractive (incoherent) dijets are sensitive to the quadrupole and dipole-dipole correlators of lightlike Wilson lines, respectively. These are among the fundamental objects describing the gluon structure at small x.

We present the first evaluation of inclusive and incoherent diffractive dijet cross sections and their azimuthal anisotropies for general small-x kinematics in the color glass condensate (CGC) effective field theory (EFT) [20,21], at leading order in α_s, resumming all terms $\sim\alpha_s \ln 1/x$. For inclusive dijets, our results explicitly validate the CLA in the kinematic region $|\boldsymbol{P}| \gg |\boldsymbol{\Delta}|$ and extend our knowledge of dijet production to the region $|\boldsymbol{P}| \lesssim |\boldsymbol{\Delta}|$, where deviations from the CLA turn out to be large. We further show that corrections to the CLA also become important when $|\boldsymbol{P}| \lesssim Q_s$, even when $|\boldsymbol{P}| > |\boldsymbol{\Delta}|$ holds. These corrections, enhanced by the saturation scale Q_s, probe genuine multigluon correlations [22,23], and are not encompassed by the resummed kinematic twists of the improved TMD framework [24] (see also [25–30] for forward dijets in dilute-dense hadronic collisions, and experimental measurements from Relativistic Heavy Ion Collider [31,32]).

Calculations of the elliptic anisotropy employing multigluon correlators deviate strongly from the CLA for $|\boldsymbol{P}| \lesssim |\boldsymbol{\Delta}|$. In particular, for transverse photon polarization the calculated elliptic modulation is qualitatively different from that in the CLA, as a maximum appears both as a function of $|\boldsymbol{P}|$ and $|\boldsymbol{\Delta}|$.

For the first time within the CGC EFT (see also [33–35]), we predict the incoherent diffractive cross section. Our calculation predicts characteristic features of the cross section's elliptic anisotropy as a function of $|\boldsymbol{P}|$ and $|\boldsymbol{\Delta}|$, involving sign changes and minima, which should be observable experimentally.

We compute the fraction of diffractive dijet events as a function of the mean dijet momentum. It increases with the mass number of the nucleus and decreases with Q^2 at a slower rate than expected in the small dipole expansion, signaling gluon saturation [36].

Dijet production in high energy DIS.—In the dipole picture of high energy deeply inelastic scattering (DIS), the

production of a forward $q-\bar{q}$ dijet can be seen as the splitting of a virtual photon γ^* into a quark-antiquark dipole and its subsequent eikonal scattering off the target's color field. We work in light-cone coordinates, and in a frame in which the virtual photon and nucleon in the target have zero transverse momenta [37]. The photon has virtuality Q^2 and four momentum $q^\mu = (-Q^2/2q^-, q^-, \mathbf{0})$. Neglecting its mass, the nucleon has energy E_n and four momentum $P_n^\mu = (\sqrt{2}E_n, 0, \mathbf{0})$. The center of mass energy of the virtual photon-nucleon system is W. The transverse momenta of the outgoing quark and antiquark are $\boldsymbol{p}_1$ and $\boldsymbol{p}_2$, their longitudinal momentum fractions are z_1 and z_2, with $z_i = p_i^-/q^- = 2E_n|\boldsymbol{p}_i|e^{-y_i}/W^2$, where p_i^- and y_i are the quark and antiquark longitudinal momenta and rapidities in this frame, respectively.

Expressed using the momenta $\boldsymbol{P} = z_2\boldsymbol{p}_1 - z_1\boldsymbol{p}_2$ and $\boldsymbol{\Delta} = \boldsymbol{p}_1 + \boldsymbol{p}_2$, at leading order in α_s, the cross sections for dijet production of massless quarks for longitudinal (L) and transverse (T) photon polarization read [9,16,38]

$$\frac{d\sigma_L^{\gamma^* A\to q\bar{q}X}}{dy_1 dy_2 d^2\boldsymbol{P} d^2\boldsymbol{\Delta}} = \frac{8\alpha_e Z_f^2 N_c S_\perp}{(2\pi)^6}\delta_z z_1^3 z_2^3 Q^2 \int_{\substack{b-b'\\ r,r'}} e^{-i\boldsymbol{P}\cdot(\boldsymbol{r}-\boldsymbol{r}')} e^{-i\boldsymbol{\Delta}\cdot(\boldsymbol{b}-\boldsymbol{b}')} \mathcal{O}_{\boldsymbol{r},\boldsymbol{b};\boldsymbol{r}',\boldsymbol{b}'} K_0(\varepsilon_f|\boldsymbol{r}|)K_0(\varepsilon_f|\boldsymbol{r}'|), \tag{1}$$

$$\frac{d\sigma_T^{\gamma^* A\to q\bar{q}X}}{dy_1 dy_2 d^2\boldsymbol{P} d^2\boldsymbol{\Delta}} = \frac{2\alpha_e Z_f^2 N_c S_\perp}{(2\pi)^6}\delta_z z_1 z_2 (z_1^2+z_2^2)\varepsilon_f^2 \int_{\substack{b-b'\\ r,r'}} e^{-i\boldsymbol{P}\cdot(\boldsymbol{r}-\boldsymbol{r}')} e^{-i\boldsymbol{\Delta}\cdot(\boldsymbol{b}-\boldsymbol{b}')} \mathcal{O}_{\boldsymbol{r},\boldsymbol{b};\boldsymbol{r}',\boldsymbol{b}'} \frac{\boldsymbol{r}\cdot\boldsymbol{r}'}{|\boldsymbol{r}||\boldsymbol{r}'|} K_1(\varepsilon_f|\boldsymbol{r}|)K_1(\varepsilon_f|\boldsymbol{r}'|). \tag{2}$$

Here, $\alpha_e = e^2/(4\pi)$ is the electromagnetic coupling, $N_c = 3$ is the number of colors, $\delta_z = \delta(1-z_1-z_2)$, $\varepsilon_f^2 = z_1 z_2 Q^2$, and $\int_{\boldsymbol{x}} = \int d^2\boldsymbol{x}$. We use $Z_f^2 = (\frac{2}{3})^2 + (-\frac{1}{3})^2 + (-\frac{1}{3})^2$, corresponding to u, d, and s quarks. Assuming a homogeneous target, the cross section is proportional to the effective transverse area of the target $S_\perp$. The multigluon correlations are encoded in $\mathcal{O}$, defined as

$$\mathcal{O}^{(4)}_{\boldsymbol{r},\boldsymbol{b};\boldsymbol{r}',\boldsymbol{b}'} = 1 - S^{(2)}_{\boldsymbol{x}_1,\boldsymbol{x}_2} - S^{(2)}_{\boldsymbol{x}_2',\boldsymbol{x}_1'} + S^{(4)}_{\boldsymbol{x}_1,\boldsymbol{x}_2;\boldsymbol{x}_2',\boldsymbol{x}_1'}, \tag{3}$$

for inclusive production, and

$$\mathcal{O}^{(2,2)}_{\boldsymbol{r},\boldsymbol{b};\boldsymbol{r}',\boldsymbol{b}'} = 1 - S^{(2)}_{\boldsymbol{x}_1,\boldsymbol{x}_2} - S^{(2)}_{\boldsymbol{x}_2',\boldsymbol{x}_1'} + S^{(2,2)}_{\boldsymbol{x}_1,\boldsymbol{x}_2;\boldsymbol{x}_2',\boldsymbol{x}_1'}, \tag{4}$$

for total diffractive (color singlet) production. The $\boldsymbol{x}$ coordinates are related to $\boldsymbol{r}$ and $\boldsymbol{b}$ via $\boldsymbol{x}_{1,2} = \boldsymbol{b} \pm z_{2,1}\boldsymbol{r}$ and $\boldsymbol{x}'_{1,2} = \boldsymbol{b}' \pm z_{2,1}\boldsymbol{r}'$. The dipole, dipole-dipole, and quadrupole correlators of fundamental lightlike Wilson lines V are defined by [9,39]

$$S^{(2)}_{\boldsymbol{x}_1,\boldsymbol{x}_2} = \frac{1}{N_c}\langle \mathrm{tr}(V^\dagger_{\boldsymbol{x}_1} V_{\boldsymbol{x}_2})\rangle, \tag{5}$$

$$S^{(2,2)}_{\boldsymbol{x}_1,\boldsymbol{x}_2;\boldsymbol{x}_2',\boldsymbol{x}_1'} = \frac{1}{N_c^2}\langle \mathrm{tr}(V^\dagger_{\boldsymbol{x}_1} V_{\boldsymbol{x}_2})\mathrm{tr}(V^\dagger_{\boldsymbol{x}_2'} V_{\boldsymbol{x}_1'})\rangle, \tag{6}$$

$$S^{(4)}_{\boldsymbol{x}_1,\boldsymbol{x}_2;\boldsymbol{x}_2',\boldsymbol{x}_1'} = \frac{1}{N_c}\langle \mathrm{tr}(V^\dagger_{\boldsymbol{x}_1} V_{\boldsymbol{x}_2} V^\dagger_{\boldsymbol{x}_2'} V_{\boldsymbol{x}_1'})\rangle, \tag{7}$$

where the $\langle\cdot\rangle$ denote the average over static large x color source configurations in the CGC EFT.

The correlators $\mathcal{O}_{\boldsymbol{r},\boldsymbol{b};\boldsymbol{r}',\boldsymbol{b}'}$ contain both the elastic and inelastic parts. In this Letter we neglect the impact parameter dependence of the target such that the elastic cross section vanishes at nonzero $\boldsymbol{\Delta}$. In this case Eqs. 3 and 4 can be simplified by subtracting the elastic piece [40], which amount to the replacements $\mathcal{O}^{(4)}_{\boldsymbol{r},\boldsymbol{b};\boldsymbol{r}',\boldsymbol{b}'} \to S^{(4)}_{\boldsymbol{x}_1,\boldsymbol{x}_2;\boldsymbol{x}_2',\boldsymbol{x}_1'} - S^{(2)}_{\boldsymbol{x}_1,\boldsymbol{x}_2}S^{(2)}_{\boldsymbol{x}_2',\boldsymbol{x}_1'}$, and $\mathcal{O}^{(2,2)}_{\boldsymbol{r},\boldsymbol{b};\boldsymbol{r}',\boldsymbol{b}'} \to S^{(2,2)}_{\boldsymbol{x}_1,\boldsymbol{x}_2;\boldsymbol{x}_2',\boldsymbol{x}_1'} - S^{(2)}_{\boldsymbol{x}_1,\boldsymbol{x}_2}S^{(2)}_{\boldsymbol{x}_2',\boldsymbol{x}_1'}$.

The correlators above are evaluated at $x = (Q^2 + |\boldsymbol{\Delta}|^2 + M^2_{q\bar{q}})/W^2$, which follows from kinematics and energy-momentum conservation [9,19], where the invariant mass of the dijet is given by $M^2_{q\bar{q}} = |\boldsymbol{P}|^2/(z_1 z_2)$.

To reduce the computational cost of our calculation, we employ the nonlinear Gaussian approximation [9,39,41–44], which allows one to express any n-point correlator of lightlike Wilson lines as a nonlinear function of the dipole correlator in Eq. (5), and was shown to approximate the full quadrupole operator very well [41,45], even after Jalilian-Marian, Iancu, McLerran, Weigert, Leonidov and Kovner (JIMWLK) small x evolution [46–52] for many units in rapidity. Gaussian approximation expressions for the dipole-dipole and quadrupole correlators are given in [9,39] and are summarized in [53]. For the dipole correlator we use the solution of the running coupling Balitsky-Kovchegov (BK) equation [58–60] with McLerran-Venugopalan model initial conditions [61]. The parameters were obtained by fitting HERA deep inelastic scattering data [62] (see [63] and [53] for details).

Cross section and elliptic anisotropy.—We present results for the angle averaged cross section and elliptic anisotropy for inclusive and diffractive dijet production in the scattering of longitudinally and transversely polarized photons with virtuality $Q^2 = 10\ \mathrm{GeV}^2$ off nuclear targets and center of mass energy of the photon-nucleon system $W = 90$ GeV. These are defined as follows [64]:

$$\frac{d\sigma^{\gamma^* A\to q\bar{q}X}_{L/T}}{d\Pi} = \int \frac{d\theta_{\boldsymbol{P}}}{2\pi}\frac{d\theta_{\boldsymbol{\Delta}}}{2\pi}\frac{d\sigma^{\gamma^* A\to q\bar{q}X}_{L/T}}{dy_1 dy_2 d^2\boldsymbol{P} d^2\boldsymbol{\Delta}}, \tag{8}$$

and

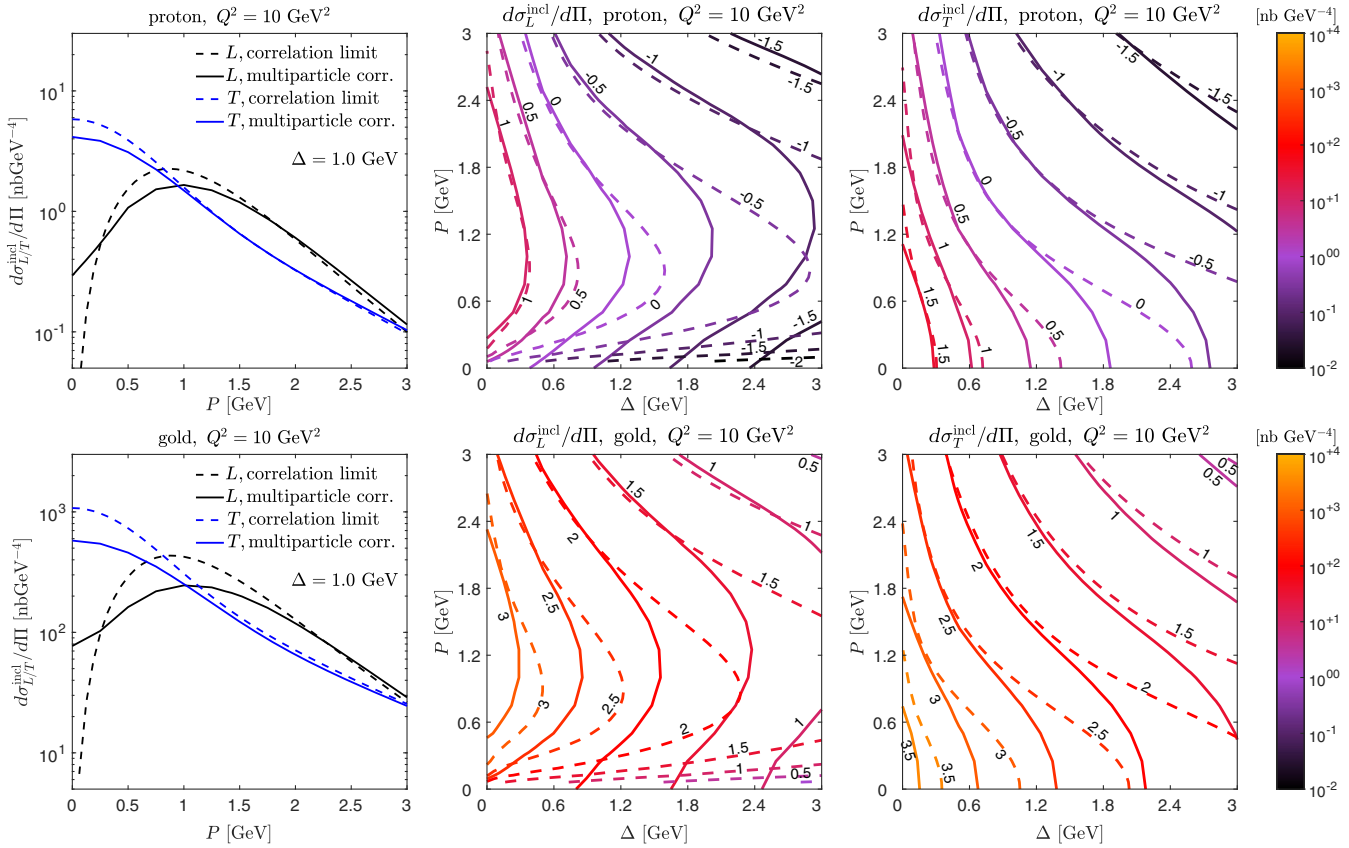

FIG. 1. Angle averaged inclusive dijet cross section for proton (upper) and gold (lower) targets. Solid lines: full multiparticle correlator result. Dashed lines: CLA. Contour labels represent powers of 10. Panels on the left show a vertical section of the contour plots at fixed $|\boldsymbol{\Delta}| = 1$ GeV.

$$v_{2,L/T}^{\gamma^* A\to q\bar{q}X} = \frac{\int \frac{d\theta_{\boldsymbol{P}}}{2\pi}\frac{d\theta_{\boldsymbol{\Delta}}}{2\pi} e^{i2(\theta_{\boldsymbol{P}}-\theta_{\boldsymbol{\Delta}})} \frac{d\sigma_{L/T}^{\gamma^* A\to q\bar{q}X}}{dy_1 dy_2 d^2\boldsymbol{P} d^2\boldsymbol{\Delta}}}{\int \frac{d\theta_{\boldsymbol{P}}}{2\pi}\frac{d\theta_{\boldsymbol{\Delta}}}{2\pi} \frac{d\sigma_{L/T}^{\gamma^* A\to q\bar{q}X}}{dy_1 dy_2 d^2\boldsymbol{P} d^2\boldsymbol{\Delta}}}. \tag{9}$$

We study proton and gold targets and in the inclusive case compare to the CLA. Additionally, we predict the ratio of diffractive to inclusive events as a function of dijet momentum for different targets and Q^2. All results are for fixed $z_1 = z_2 = 0.5$.

Inclusive dijets: In Fig. 1 we show the angle averaged cross sections, comparing results using full multiparticle correlators Eqs. (1) and (2) (solid lines) to the CLA [18,19,53] (dashed lines). The former are valid for any value of $\boldsymbol{\Delta}$, while the latter are expected to be valid only for $|\boldsymbol{P}| \gg |\boldsymbol{\Delta}|$. The expected agreement between the CLA and the more general result at $|\boldsymbol{P}| \gg |\boldsymbol{\Delta}|$ is clearly confirmed in all cases. Deviations from the CLA become large when extrapolated to the regime $|\boldsymbol{\Delta}| > |\boldsymbol{P}|$.

Importantly, we observe significant deviations from the CLA at $|\boldsymbol{\Delta}| < |\boldsymbol{P}| < 1.5$ GeV for the gold target, and much milder deviations for the proton. This difference is explained by saturation effects: the cross sections beyond the CLA receive genuine saturation corrections of order $Q_s^2/|\boldsymbol{P}|^2$ and Q_s^2/Q^2, in addition to kinematic corrections of order $|\boldsymbol{\Delta}|^2/|\boldsymbol{P}|^2$ [22,23]. This observation demonstrates that inclusive dijet production in $e + A$ collisions at a future EIC can provide direct access to gluon saturation.

In Fig. 2 we present the elliptic modulation of the cross section in the angle between $\boldsymbol{P}$ and $\boldsymbol{\Delta}$. Again, the CLA provides a good estimate in the region $|\boldsymbol{P}| \gg |\boldsymbol{\Delta}|$, and deviations become large for $|\boldsymbol{\Delta}| \gtrsim |\boldsymbol{P}|$. We predict a minimum $v_{2T} \sim -30\%$ for proton targets in the range $|\boldsymbol{P}| \sim |\boldsymbol{\Delta}| \sim$ 1.8 GeV, and $v_{2T} \sim -20\%$ for gold for $|\boldsymbol{P}| \sim |\boldsymbol{\Delta}| \sim$ 2.2 GeV, unlike the CLA, which predicts decreasing values of v_{2T} as $|\boldsymbol{\Delta}|$ increases [53]. To probe these, and the aforementioned saturation effects, experiments should focus on the kinematics $|\mathbf{P}| \sim |\boldsymbol{\Delta}|$. We further confirm the large elliptic modulation for the longitudinally polarized photon, which was obtained previously in the CLA [18,19,53].

Diffractive dijets: We show results of diffractive dijet cross sections and elliptic anisotropies for virtual photon off gold scattering in Fig. 3. Although our results contain only incoherent diffraction, these are the most dominant at momentum transfer $|\boldsymbol{\Delta}| \gtrsim 1/R_A (\sim 0.2$ GeV for gold), such that the result is approximately equal to the total diffractive cross section.

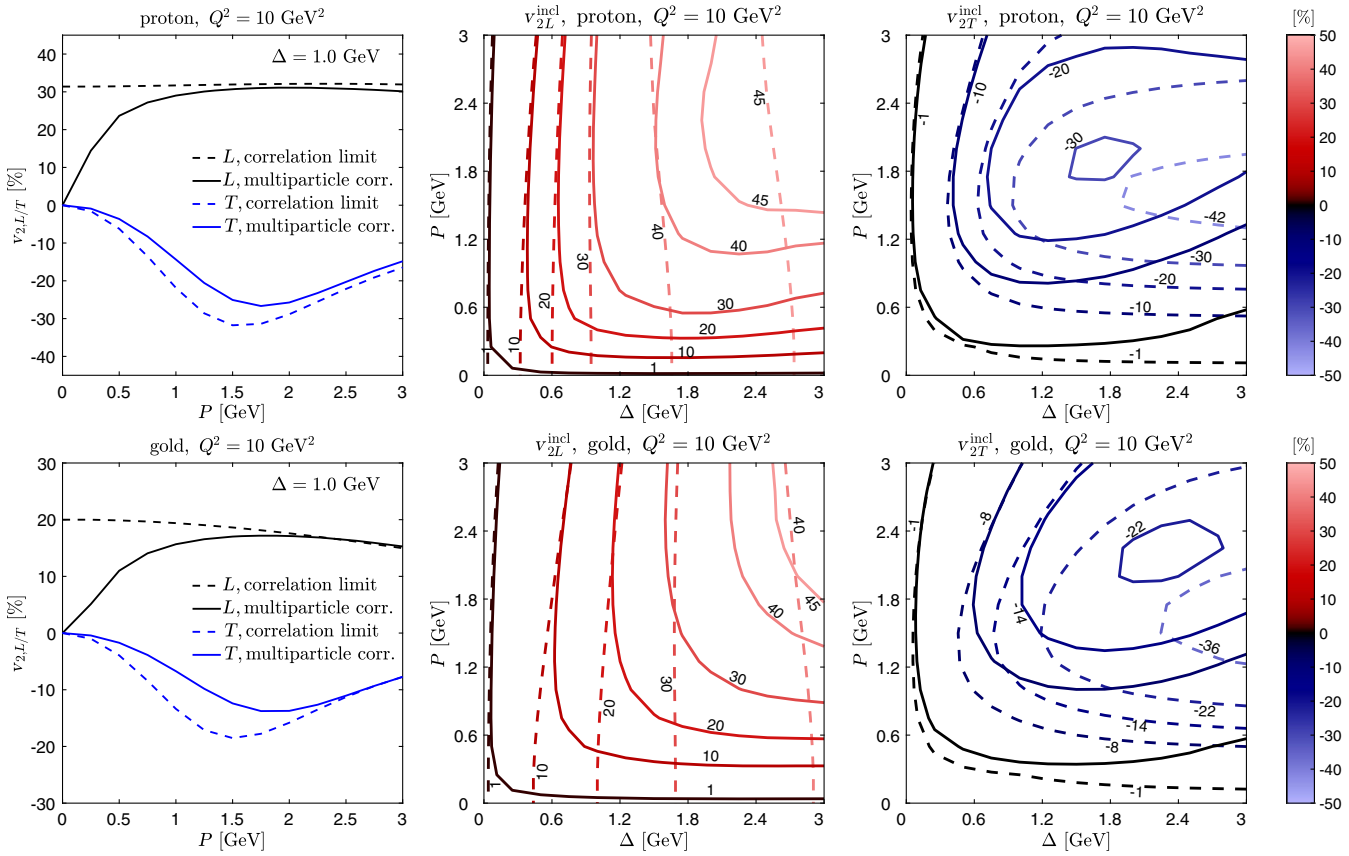

FIG. 2. Elliptic anisotropy of inclusive dijet cross sections for proton (upper), and gold (lower). Solid lines: full multiparticle correlator result. Dashed lines: CLA. Panels on the left show a vertical section of the contour plots at fixed $|\boldsymbol{\Delta}| = 1$ GeV. We emphasize the appearance of distinct minima in the v_{2T}, which are not captured by the CLA.

Comparing the inclusive (Fig. 1) and diffractive cross sections (Fig. 3), we observe a strong suppression of diffractive events and a different $|\boldsymbol{P}|$ dependence for the longitudinal and transverse cases. Theoretically, this can be directly related to the properties of multigluon correlators in the target. The only difference between the inclusive and diffractive cross sections are the different color structures of the correlators $\mathcal{O}$ (Eqs. 3 and 4). A small dipole expansion explains the effect of this difference. The first nonvanishing term in the expansion occurs at linear order for the inclusive case and at quadratic order for diffractive production, because diffractive events require at least two gluons exchanged in the amplitude to ensure color neutrality.

The elliptic modulation of the incoherent diffractive cross section is shown in the middle panel of Fig. 3. For both polarizations it exhibits a sign change as a function of $|\boldsymbol{P}|$, similar to that observed in coherent diffractive dijet production [6,7]. The transverse case also shows a sign change in $|\boldsymbol{\Delta}|$ for $|\boldsymbol{P}| \gtrsim 2$ GeV. Importantly, the elliptic modulation reaches large values (tens of percent) in the studied kinematic range.

In the right panels of Fig. 3 we show the ratio of diffractive to inclusive events as a function of $|\boldsymbol{P}|$ for fixed $|\boldsymbol{\Delta}| = 1.5$ GeV. The fraction of diffractive events increases with the target saturation scale Q_s from proton to gold, and decreases with increasing photon virtuality Q^2. An expansion in small dipoles predicts the fraction of diffractive events to increase as Q_s^2. We expect a factor of 2.6 increase in the considered kinematics after BK evolution from proton to gold; however, we find a smaller increase of 1.9 (2.3) for transversely (longitudinally) polarized photons at $|\boldsymbol{P}| \approx 1$ GeV and $Q^2 = 4$ GeV^2, with a mild increase towards the expected value of 2.6 with growing $|\boldsymbol{P}|$. This behavior indicates effects of gluon saturation, which are stronger in larger nuclei. We argue that this ratio is a key measurement at a future EIC, allowing to quantify gluon saturation (differentially in $|\boldsymbol{P}|$ and Q^2).

Conclusions.—We computed inclusive and (incoherent) diffractive dijet production cross sections in $e + p$ and $e + A$ collisions at a future EIC within the CGC EFT. These cross sections are sensitive probes of multigluon correlations inside nuclear targets at small x and allow to quantitatively probe gluon saturation experimentally.

Our approach is not restricted to $|\boldsymbol{P}| \gg |\boldsymbol{\Delta}|$ and significantly increases the theoretically accessible kinematic range. We employed the nonlinear Gaussian approximation, using dipole correlators obtained from running

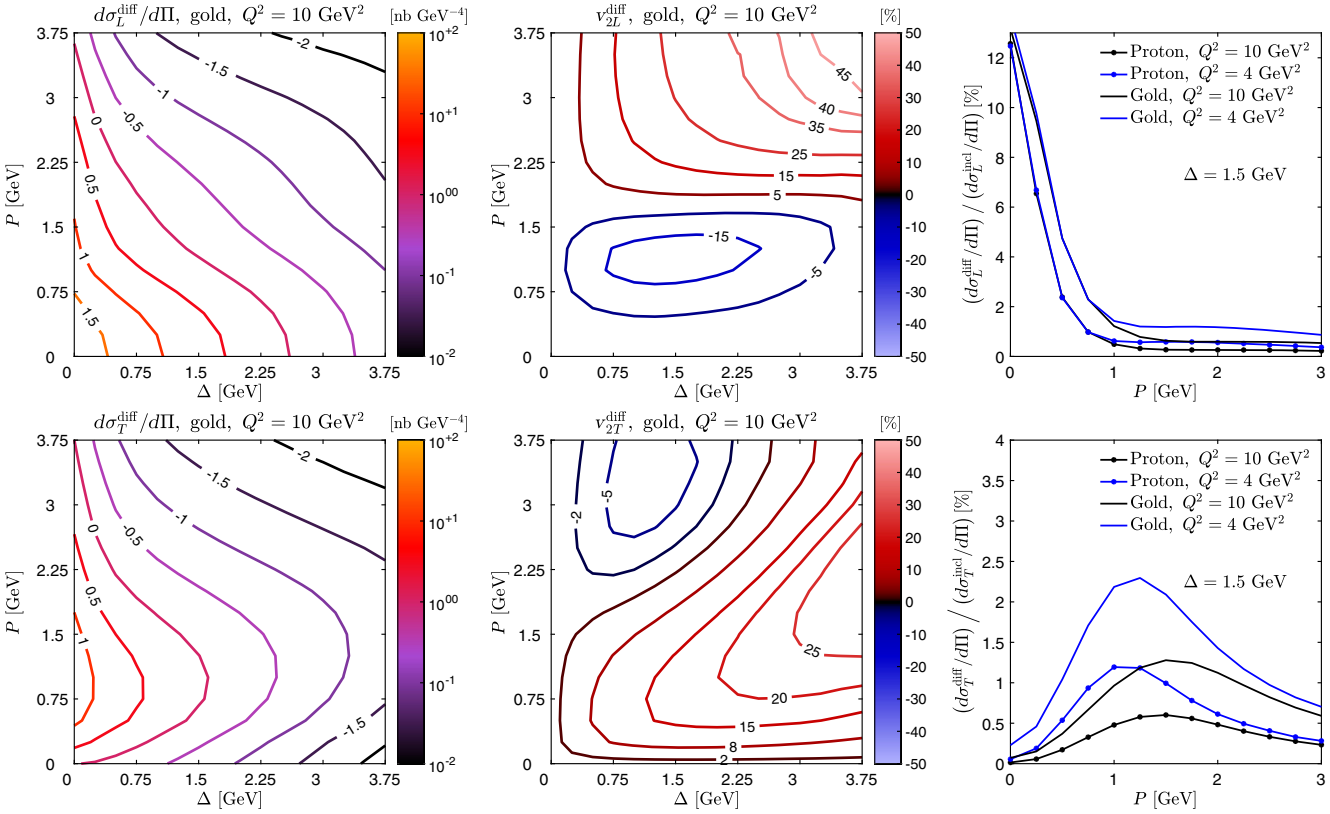

FIG. 3. Left: diffractive angle averaged dijet cross sections (contour labels represent powers of 10). Center: diffractive elliptic anisotropy. Right: ratio diffractive to inclusive cross section. Upper panels: longitudinal. Lower panels: transverse.

coupling BK fits to HERA data. We validated the CLA in inclusive dijet production for most $|\boldsymbol{P}| \gg |\boldsymbol{\Delta}|$, but found significant target dependent corrections for $|\boldsymbol{P}| \lesssim |\boldsymbol{\Delta}|$ or $|\boldsymbol{P}| \lesssim Q_s$, the latter being caused by gluon saturation effects. We thus argue that the regime of moderate $|\boldsymbol{P}| \sim Q_s$ of the target is particularly interesting when studying dijet production at a future EIC. Differential measurements in $\boldsymbol{P}$ and $\boldsymbol{\Delta}$ within a range that includes Q_s will allow to reveal the complex multiparton structure of nuclei and uncover saturation.

We presented the first calculation of diffractive dijet cross sections and their elliptic modulation within the CGC EFT. We studied the nuclear modification of the ratio between the differential inclusive and diffractive dijet cross sections by comparing gold to proton targets, and at different values of Q^2. The dependence of the ratio between the cross sections on the target's saturation momentum indicates that saturation effects are significant in the studied kinematic regime.

In future work, we plan to include parton showers, hadronization, and full jet reconstruction. Based on results in [19], we expect the v_2 of the produced $q - \bar{q}$ pair presented here to be a good estimator of the observable dijet v_2. It will also be important to include next-to-leading order (NLO) corrections, both in small-x evolution equations: NLO BK [65–68] or NLO JIMWLK [69,70], and the NLO impact factor [71–75], and to consider the effects of soft gluon radiation of the final state jets that is not captured by the jet algorithm [8].

Detailed extraction of multi-gluon correlators in nuclei and experimental confirmation of gluon saturation will likely require complex global fits to a wide variety of experimental data. We have demonstrated that inclusive and diffractive dijet production are two of the most important processes to consider.

We thank Elke-Caroline Aschenauer, Renaud Boussarie, Kaushik Roy, Sören Schlichting, Vladimir Skokov, Alba Soto-Ontoso, and Raju Venugopalan for useful discussions. H. M. is supported by the Academy of Finland Project No. 314764. N. M., F. S., and B. S. are supported under DOE Contract No. DE-SC0012704. N. M. is funded by the Deutsche Forschungsgemeinschaft (DFG, German Research Foundation), Project No. 404640738. This research used resources of the National Energy Research Scientific Computing Center, which is supported by the Office of Science of the U.S. Department of Energy under Contract No. DE-AC02-05CH11231.

*heikki.mantysaari@jyu.fi
†nmueller@bnl.gov
‡farid.salazarwong@stonybrook.edu
§bschenke@bnl.gov

[1] D. Boer *et al.*, Gluons and the quark sea at high energies: Distributions, polarization, tomography, arXiv:1108.1713.

[2] A. Accardi *et al.*, Electron-ion collider: The next QCD frontier, Eur. Phys. J. A **52**, 268 (2016).

[3] E. C. Aschenauer, S. Fazio, J. H. Lee, H. Mäntysaari, B. S. Page, B. Schenke, T. Ullrich, R. Venugopalan, and P. Zurita, The electron–ion collider: Assessing the energy dependence of key measurements, Rep. Prog. Phys. **82**, 024301 (2019).

[4] T. Altinoluk, N. Armesto, G. Beuf, and A. H. Rezaeian, Diffractive dijet production in deep inelastic scattering and photon-hadron collisions in the color glass condensate, Phys. Lett. B **758**, 373 (2016).

[5] Y. Hatta, B.-W. Xiao, and F. Yuan, Probing the Small-x Gluon Tomography in Correlated Hard Diffractive Dijet Production in Deep Inelastic Scattering, Phys. Rev. Lett. **116**, 202301 (2016).

[6] H. Mäntysaari, N. Mueller, and B. Schenke, Diffractive dijet production and Wigner distributions from the color glass condensate, Phys. Rev. D **99**, 074004 (2019).

[7] F. Salazar and B. Schenke, Diffractive dijet production in impact parameter dependent saturation models, Phys. Rev. D **100**, 034007 (2019).

[8] Y. Hatta, N. Mueller, T. Ueda, and F. Yuan, QCD resummation in hard diffractive dijet production at the electron-ion collider, Phys. Lett. B **802**, 135211 (2020).

[9] F. Dominguez, C. Marquet, B.-W. Xiao, and F. Yuan, Universality of unintegrated gluon distributions at small x, Phys. Rev. D **83**, 105005 (2011).

[10] A. H. Mueller, B.-W. Xiao, and F. Yuan, Sudakov double logarithms resummation in hard processes in the small-x saturation formalism, Phys. Rev. D **88**, 114010 (2013).

[11] H. Mäntysaari and B. Schenke, Evidence of Strong Proton Shape Fluctuations from Incoherent Diffraction, Phys. Rev. Lett. **117**, 052301 (2016).

[12] H. Mäntysaari and B. Schenke, Revealing proton shape fluctuations with incoherent diffraction at high energy, Phys. Rev. D **94**, 034042 (2016).

[13] H. Mäntysaari and B. Schenke, Probing subnucleon scale fluctuations in ultraperipheral heavy ion collisions, Phys. Lett. B **772**, 832 (2017).

[14] H. Mäntysaari and B. Schenke, Confronting impact parameter dependent JIMWLK evolution with HERA data, Phys. Rev. D **98**, 034013 (2018).

[15] H. Mäntysaari and B. Schenke, Accessing the gluonic structure of light nuclei at the electron-ion collider, Phys. Rev. C **101**, 015203 (2020).

[16] F. Dominguez, J.-W. Qiu, B.-W. Xiao, and F. Yuan, On the linearly polarized gluon distributions in the color dipole model, Phys. Rev. D **85**, 045003 (2012).

[17] A. Metz and J. Zhou, Distribution of linearly polarized gluons inside a large nucleus, Phys. Rev. D **84**, 051503(R) (2011).

[18] A. Dumitru, T. Lappi, and V. Skokov, Distribution of Linearly Polarized Gluons and Elliptic Azimuthal Anisotropy in Deep Inelastic Scattering Dijet Production at High Energy, Phys. Rev. Lett. **115**, 252301 (2015).

[19] A. Dumitru, V. Skokov, and T. Ullrich, Measuring the Weizsäcker-Williams distribution of linearly polarized gluons at an electron-ion collider through dijet azimuthal asymmetries, Phys. Rev. C **99**, 015204 (2019).

[20] F. Gelis, E. Iancu, J. Jalilian-Marian, and R. Venugopalan, The color glass condensate, Annu. Rev. Nucl. Part. Sci. **60**, 463 (2010).

[21] E. Iancu and R. Venugopalan, The color glass condensate and high-energy scattering in QCD Quark-Gluon Plasma **3**, 249 (2004).

[22] A. Dumitru and V. Skokov, $\cos(4\phi)$ azimuthal anisotropy in small-x DIS dijet production beyond the leading power TMD limit, Phys. Rev. D **94**, 014030 (2016).

[23] T. Altinoluk and R. Boussarie, Low x physics as an infinite twist (G)TMD framework: Unravelling the origins of saturation, J. High Energy Phys. 10 (2019) 208.

[24] T. Altinoluk, R. Boussarie, and P. Kotko, Interplay of the CGC and TMD frameworks to all orders in kinematic twist, J. High Energy Phys. 05 (2019) 156.

[25] C. Marquet, Forward inclusive dijet production and azimuthal correlations in pA collisions, Nucl. Phys. **A796**, 41 (2007).

[26] T. Lappi and H. Mäntysaari, Forward dihadron correlations in deuteron-gold collisions with the Gaussian approximation of JIMWLK, Nucl. Phys. **A908**, 51 (2013).

[27] E. Iancu and J. Laidet, Gluon splitting in a shockwave, Nucl. Phys. **A916**, 48 (2013).

[28] P. Kotko, K. Kutak, C. Marquet, E. Petreska, S. Sapeta, and A. van Hameren, Improved TMD factorization for forward dijet production in dilute-dense hadronic collisions, J. High Energy Phys. 09 (2015) 106.

[29] A. van Hameren, P. Kotko, K. Kutak, C. Marquet, E. Petreska, and S. Sapeta, Forward di-jet production in p + Pb collisions in the small-x improved TMD factorization framework, J. High Energy Phys. 12 (2016) 034; J. High Energy Phys. 02 (2019) 158.

[30] J. L. Albacete, G. Giacalone, C. Marquet, and M. Matas, Forward dihadron back-to-back correlations in pA collisions, Phys. Rev. D **99**, 014002 (2019).

[31] A. Adare *et al.* (PHENIX Collaboration), Suppression of Back-to-Back Hadron Pairs at Forward Rapidity in d + Au Collisions at $\sqrt{s_{NN}} = 200$ GeV, Phys. Rev. Lett. **107**, 172301 (2011).

[32] E. Braidot, Two-particle azimuthal correlations at forward rapidity in STAR, Ph.D. thesis, Utrecht U., 2011.

[33] A. Aktas *et al.* (H1 Collaboration), Tests of QCD factorisation in the diffractive production of dijets in deep-inelastic scattering and photoproduction at HERA, Eur. Phys. J. C **51**, 549 (2007).

[34] V. Guzey and M. Klasen, A fresh look at factorization breaking in diffractive photoproduction of dijets at HERA at next-to-leading order QCD, Eur. Phys. J. C **76**, 467 (2016).

[35] I. Helenius and C. O. Rasmussen, Hard diffraction in photoproduction with Pythia 8, Eur. Phys. J. C **79**, 413 (2019).

[36] H. Kowalski, T. Lappi, C. Marquet, and R. Venugopalan, Nuclear enhancement and suppression of diffractive structure functions at high energies, Phys. Rev. C **78**, 045201 (2008).

[37] We denote 2D transverse vectors as $\boldsymbol{x}$, with magnitude $|\boldsymbol{x}|$.

[38] K. Roy and R. Venugopalan, Inclusive prompt photon production in electron-nucleus scattering at small x, J. High Energy Phys. 05 (2018) 013.

[39] T. Lappi, B. Schenke, S. Schlichting, and R. Venugopalan, Tracing the origin of azimuthal gluon correlations in the color glass condensate, J. High Energy Phys. 01 (2016) 061.

[40] The elastic (coherent) production of dijets is given by Eqs. (1) and (2) with $\mathcal{O}_{\boldsymbol{r},\boldsymbol{b};\boldsymbol{r}',\boldsymbol{b}'}=1-S^{(2)}_{\boldsymbol{x}_1,\boldsymbol{x}_2}-S^{(2)}_{\boldsymbol{x}'_2,\boldsymbol{x}'_1}+S^{(2)}_{\boldsymbol{x}_1,\boldsymbol{x}_2}S^{(2)}_{\boldsymbol{x}'_2,\boldsymbol{x}'_1}$.

[41] A. Dumitru, J. Jalilian-Marian, T. Lappi, B. Schenke, and R. Venugopalan, Renormalization group evolution of multi-gluon correlators in high energy QCD, Phys. Lett. B **706**, 219 (2011).

[42] F. Dominguez, C. Marquet, and B. Wu, On multiple scatterings of mesons in hot and cold QCD matter, Nucl. Phys. **A823**, 99 (2009).

[43] J. P. Blaizot, F. Gelis, and R. Venugopalan, High-energy pA collisions in the color glass condensate approach. 2. Quark production, Nucl. Phys. **A743**, 57 (2004).

[44] K. Fukushima and Y. Hidaka, Light projectile scattering off the color glass condensate, J. High Energy Phys. 06 (2007) 040.

[45] E. Iancu and D. N. Triantafyllopoulos, JIMWLK evolution in the Gaussian approximation, J. High Energy Phys. 04 (2012) 025.

[46] J. Jalilian-Marian, A. Kovner, L. D. McLerran, and H. Weigert, The intrinsic glue distribution at very small x, Phys. Rev. D **55**, 5414 (1997).

[47] J. Jalilian-Marian, A. Kovner, A. Leonidov, and H. Weigert, The Wilson renormalization group for low x physics: Towards the high density regime, Phys. Rev. D **59**, 014014 (1998).

[48] J. Jalilian-Marian, A. Kovner, A. Leonidov, and H. Weigert, The BFKL equation from the Wilson renormalization group, Nucl. Phys. **B504**, 415 (1997).

[49] E. Iancu, A. Leonidov, and L. D. McLerran, The Renormalization group equation for the color glass condensate, Phys. Lett. B **510**, 133 (2001).

[50] E. Iancu, A. Leonidov, and L. D. McLerran, Nonlinear gluon evolution in the color glass condensate. 1., Nucl. Phys. **A692**, 583 (2001).

[51] E. Ferreiro, E. Iancu, A. Leonidov, and L. McLerran, Nonlinear gluon evolution in the color glass condensate. 2., Nucl. Phys. **A703**, 489 (2002).

[52] E. Iancu and L. D. McLerran, Saturation and universality in QCD at small x, Phys. Lett. B **510**, 145 (2001).

[53] See the Supplemental Material at http://link.aps.org/supplemental/10.1103/PhysRevLett.124.112301 for Gaussian approximation, dipole amplitude, and correlation limit approximation (CLA), which includes Refs. [6,54–57].

[54] T. Lappi and S. Schlichting, Linearly polarized gluons and axial charge fluctuations in the Glasma, Phys. Rev. D **97**, 034034 (2018).

[55] B. Ducloué, T. Lappi, and H. Mäntysaari, Forward J/ψ production in proton-nucleus collisions at high energy, Phys. Rev. D **91**, 114005 (2015).

[56] B. Ducloué, T. Lappi, and H. Mäntysaari, Forward J/ψ production at high energy: Centrality dependence and mean transverse momentum, Phys. Rev. D **94**, 074031 (2016).

[57] B. Ducloué, T. Lappi, and H. Mäntysaari, Forward J/ψ and D meson nuclear suppression at the LHC, Nucl. Part. Phys. Proc. **289–290**, 309 (2017).

[58] I. Balitsky, Operator expansion for high-energy scattering, Nucl. Phys. **B463**, 99 (1996).

[59] Y. V. Kovchegov, Small x F_2 structure function of a nucleus including multiple pomeron exchanges, Phys. Rev. D **60**, 034008 (1999).

[60] I. Balitsky, Quark contribution to the small-x evolution of color dipole, Phys. Rev. D **75**, 014001 (2007).

[61] L. D. McLerran and R. Venugopalan, Computing quark and gluon distribution functions for very large nuclei, Phys. Rev. D **49**, 2233 (1994).

[62] F. D. Aaron *et al.* (H1 and ZEUS Collaborations), Combined measurement and QCD analysis of the inclusive $e^{\pm}p$ scattering cross sections at HERA, J. High Energy Phys. 01 (2010) 109.

[63] T. Lappi and H. Mäntysaari, Single inclusive particle production at high energy from HERA data to proton-nucleus collisions, Phys. Rev. D **88**, 114020 (2013).

[64] The differential $d\Pi$ is defined as $(2\pi)^2|\boldsymbol{P}|d|\boldsymbol{P}||\boldsymbol{\Delta}|d|\boldsymbol{\Delta}|dy_1dy_2$.

[65] I. Balitsky and G. A. Chirilli, Next-to-leading order evolution of color dipoles, Phys. Rev. D **77**, 014019 (2008).

[66] E. Iancu, J. D. Madrigal, A. H. Mueller, G. Soyez, and D. N. Triantafyllopoulos, Resumming double logarithms in the QCD evolution of color dipoles, Phys. Lett. B **744**, 293 (2015).

[67] T. Lappi and H. Mäntysaari, Direct numerical solution of the coordinate space Balitsky-Kovchegov equation at next to leading order, Phys. Rev. D **91**, 074016 (2015).

[68] T. Lappi and H. Mäntysaari, Next-to-leading order Balitsky-Kovchegov equation with resummation, Phys. Rev. D **93**, 094004 (2016).

[69] I. Balitsky and G. A. Chirilli, Rapidity evolution of Wilson lines at the next-to-leading order, Phys. Rev. D **88**, 111501(R) (2013).

[70] A. Kovner, M. Lublinsky, and Y. Mulian, Jalilian-Marian, Iancu, McLerran, Weigert, Leonidov, Kovner evolution at next to leading order, Phys. Rev. D **89**, 061704(R) (2014).

[71] R. Boussarie, A. V. Grabovsky, D. Yu. Ivanov, L. Szymanowski, and S. Wallon, Next-to-Leading Order Computation of Exclusive Diffractive Light Vector Meson Production in a Saturation Framework, Phys. Rev. Lett. **119**, 072002 (2017).

[72] G. Beuf, Dipole factorization for DIS at NLO: Combining the $q\bar{q}$ and $q\bar{q}g$ contributions, Phys. Rev. D **96**, 074033 (2017).

[73] H. Hänninen, T. Lappi, and R. Paatelainen, One-loop corrections to light cone wave functions: The dipole picture DIS cross section, Ann. Phys. (Amsterdam) **393**, 358 (2018).

[74] K. Roy and R. Venugopalan, NLO impact factor for inclusive photon + dijet production in $e+A$ DIS at small x, arXiv:1911.04530.

[75] K. Roy and R. Venugopalan, Extracting many-body correlators of saturated gluons with precision from inclusive photon + dijet final states in deeply inelastic scattering, arXiv:1911.04519.